Simulation on non-uniform velocity dynamic crack growing by TDBEM

Zhenhan Yao, Zhihong Zhou, Bo Wang
Department of Engineering Mechanics, Tsinghua University, Beijing, 100084 China, demyzh@mail.tsinghua.edu.cn

Abstract

The time-domain dual boundary element method (TDBEM), due to its single-region feature, has been successfully used for simulating crack growth problem [1]. However the previous work pay little attention to weakly singular integration in TDBEM, which may result in error about several percent [6]. To improve the accuracy of numerical integration, first, the quadratic or biquadratic equations have been derived to find out weakly singular points in an element, and the element is divided into several integration sections according to the singular points. Each section only has one singular point at the end. Then, a function transformation has been introduced into weakly singular integration of each section to eliminate the singularity. The method is turned out to be simple and the effort needed in programming is little. To show that the whole procedure is correct, a comparison of calculation results with experimental data has been carried out. The experimental data on polystyrene crack growth given by Papadopoulos [5] have been chosen as the original data, and they have been carefully analyzed by using the elasto-plastic FEM and simulating the caustic method. The results revealed that if the size of plastic zone around the crack tip has the same order with measured spot, the stress intensity factors (S F) calculated by elastic formulation will deviate from the real values significantly, and have to be corrected. Finally, after comparing SIFs from TDBEM with experimental data, it shows that these two results are in good agreement.

1 Introduction

The initiation, propagation and bifurcation depend on the magnitude and distribution of the stress and strain around the crack tip. Under condition of small

yield range, the stress and strain fields are controlled by the dynamic stress intensity factor.

In numerical analysis of fracture problem, limitation of finite element method to solve the problem of crack growth is that the growth path of crack should be known in advance, or re-meshing is necessary during the computation, which makes FEM unpopular in crack growth problems. Boundary element method, on the other hand, only needs meshing on the boundary of domain and the crack faces. When a crack is propagating, it is enough to add new elements to the crack tip.

A number of BE methods have been proposed to simulate the dynamic crack growth by researchers. Among them, Kollor et al. [3] employed BEM to study the growth of semi-infinite crack at constant velocity. Gallego and Dominguez [4] simulated crack growth by using moving singular crack element and re-meshing on boundary. Fedelinski et al. [1][2] proposed time domain dual boundary element method. They took cracked body as a single region and divided boundary including crack faces into elements. This method is more convenient than above methods in calculation of crack growth.

In this paper, TDBEM has been applied in crack growth at non-uniform velocity, and the accuracy of weakly singular integration in TDBEM has been improved by introducing function transformation.

To show the capability of TDBEM to solve dynamic crack growth at non-uniform velocity, the comparison between the results of TDBEM on crack growth and the experimental data is given. First, experimental data given by Papadopoulos [5] has been analyzed by finite element method. It is found that the dynamic stress intensity factors K_I^d given in that paper are larger than they should be, because the size of crazing zone has the same order of that of caustics and its effect on stress field of crack tip is no longer negligible. Then, modifications of the dynamic stress intensity factors are carried out according to the result of FEM simulation on caustics. Finally, comparison between the solution of TDBEM on crack growth and modified experimental data has been carried out.

2 Numerical formulation of TDBEM on dynamic crack growth

2.1 Discretization of boundary integration equations

The discretization of both space and time is required in numerical calculation. The boundary S of the body is divided into M boundary elements with Z nodes in each element. The observation time t is divided into N time steps with equal time interval. The temporal variation of boundary quantities is specified by H value within the time step. The crack propagation is simulated by adding new elements ahead of the crack tip. At a given time, the number of elements is denoted by $M(n) = M_0 + M_c(n)$, where M_0 is the initial number of elements and $M_c(n)$ is the number of newly formed elements during crack growth. The displacements and traction are approximated by interpolation

function $N^z(\xi)$ in each element and time step by interpolation function $M^h(\tau)$. After approximations, displacement and traction equations can be written as

$$c_{ij}^l u_j^{lN} = \sum_{n=1}^{N}\sum_{h=1}^{H}\sum_{m=1}^{M}\sum_{z=1}^{Z}\left\{t_j^{nhmz}\int_{-1}^{1}\left[\int_{\tau^{n-1}}^{\tau} U_{ij}^{lN}(\xi,\tau)M^h(\tau)\mathrm{d}\tau\right]N^z(\xi)J^m(\xi)\mathrm{d}\xi - u_j^{nhmz}\int_{-1}^{1}\left[\int_{\tau^{n-1}}^{\tau} T_{ij}^{lN}(\xi,\tau)M^h(\tau)\mathrm{d}\tau\right]N^z(\xi)J^m(\xi)\mathrm{d}\xi\right\},\ l=1,2,\cdots L_1 \tag{1}$$

and

$$\frac{1}{2}t_j^{lN} = n_i^l\sum_{n=1}^{N}\sum_{h=1}^{H}\sum_{m=1}^{M}\sum_{z=1}^{Z}\left\{t_k^{nhmz}\int_{-1}^{1}\left[\int_{\tau^{n-1}}^{\tau} U_{kij}^{lN}(\xi,\tau)M^h(\tau)\mathrm{d}\tau\right]N^z(\xi)J^m(\xi)\mathrm{d}\xi - u_k^{nhmz}\int_{-1}^{1}\left[\int_{\tau^{n-1}}^{\tau} T_{kij}^{lN}(\xi,\tau)M^h(\tau)\mathrm{d}\tau\right]N^z(\xi)J^m(\xi)\mathrm{d}\xi\right\},\ l=1,2,\cdots L_2 \tag{2}$$

where L_1 and L_2 are the numbers of collocation points respectively, for which the displacement and the traction equations are applied. $L = L_1 + L_2$ is the total number of nodes. J^m is the Jacobian and ξ is the local coordinate $(-1 \le \xi \le 1)$. The numbers of nodes, namely L_1, L_2 and L, increase with the crack growth. Once the positions of nodes are determined, they no longer vary with time. It should be noticed that the integrands in Equation (2) contain the expressions $1/\sqrt{1-\varphi_\alpha^2}$, which are weakly singular at the front of the wave, i.e. when $\varphi_\alpha \to 1$ [1,6].

2.2 Evaluation of the weakly singular integration

2.2.1 Search for the singular point in local coordinates

When a wave front arrives at an element, the local coordinates of the points, where the wave front are located, can be determined by

$$R = c_\alpha t \tag{3}$$

where $R = \sqrt{(x-x_p)^2 + (y-y_p)^2}$, and x_p, y_p denote the coordinates of collocation point. x, y are the coordinates of a point in the element, and they can be expressed by local coordinates:

$$\begin{aligned} x &= N_1(\xi)x_1 + N_2(\xi)x_2 + N_3(\xi)x_3 \\ y &= N_1(\xi)y_1 + N_2(\xi)y_2 + N_3(\xi)y_3 \end{aligned} \tag{4}$$

where $N_i(\xi)$ are the interpolation functions, and ξ is the local coordinate of any point in the element.
Using the following notations:

$$A=\frac{9}{8}(x_1-2x_2+x_3) \qquad B=\frac{3}{4}(x_3-x_1)$$
$$C=\frac{9}{8}(y_1-2y_2+y_3) \qquad D=\frac{3}{4}(y_3-y_1) \tag{5}$$

Equation (3) can be written as:

$$(A\xi^2+B\xi)^2+(C\xi^2+D\xi)^2+2(x_2-x_p)(A\xi^2+B\xi)$$
$$+2(y_2-y_p)(C\xi^2+D\xi)+[(x_2-x_p)^2+(y_2-y_p)^2-(c_\alpha t)^2]=0 \tag{6}$$

Suppose that the boundary of the element is straight. Therefore, the global coordinates are linear functions of the local coordinates, i.e. both A and C are equal to zero, thus the equation to obtain ξ' is reduced to a quadratic one

$$(B^2+D^2)\xi^2+2[(x_2-x_p)B+(y_2-y_p)D]\xi$$
$$+[(x_2-x_p)^2+(y_2-y_p)^2-(c_\alpha t)^2]=0 \tag{7}$$

the local coordinates of the wave front in the element can be got by equation (14), if the solution falls into the range (–1, 1). However, if the wave front arrives at a straight singular element, in which both A and C is not equal to zero, the equation becomes complicated. Let A is not equal to zero. $B/A=D/C=\beta$ (if $C\neq 0$) since all singular elements are assumed to be straight ones. Then, equation (13) can be rewritten as

$$(A^2+C^2)(\xi^2+\beta\xi)^2+2[A(x_2-x_p)+C(y_2-y_p)](\xi^2+\beta\xi)$$
$$+[(x_2-x_p)^2+(y_2-y_p)^2-(c_\alpha t)^2]=0 \tag{8}$$

the roots of the above equation can be found by solving quadratic equations twice. To get the local coordinates of the wave front in the singular element, only those values which falls into (–1, 1) are kept, and the rest are discarded.

2.2.2 Decision of the integral interval

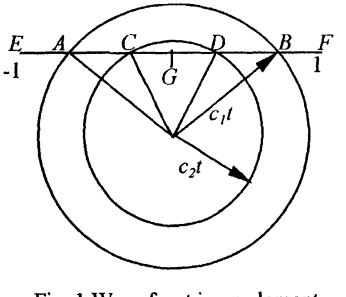

Fig. 1 Wave front in an element

After the singular points are found, integral intervals should be carefully set.

Suppose that two wave fronts have reached at an element *EF* in Fig. 1, the element is divided into five intervals.

Among five intervals: There is no singular point in *EA*; There is one singular point at *A* in *AC*; There are two singular points at *C* and *D* in *CD*; There is one singular point at *B* in *DB*; There is no singular point in BF. The *CD* section is further divided into two parts in order to make integration more convenient. Thus, all integral intervals can be classified into three kinds: (I) there is no singular point; (II) only lower limit of integration is singular; (III) only upper limit of integration is singular.

2.2.3 Evaluation of integration

Numerical integration can be easily evaluated by standard Gauss integral method if the integration interval has no singular point. However, when the low or upper limit of integration is weakly singular point, the accuracy of integration will be greatly affected if it has not been treated before numerical integration. By using function transformation $x = \sin(y)$, the weakly singular integration can be expressed as follows:

$$\int_{\xi'}^{\xi''} \frac{f(\xi)\mathrm{d}\xi}{\sqrt{1-\varphi_\alpha^2}} = \int_{\xi'}^{\xi''} \frac{g(\xi)\mathrm{d}\xi}{\sqrt{\xi-\xi^*}} = \int_{\arcsin(1+\xi'-\xi'')}^{\frac{\pi}{2}} \sqrt{1+\sin y}\, g(\xi(y))\mathrm{d}y \tag{9}$$

where $g(\xi)$ is a function without singularity in (ξ', ξ''). If the lower limit of integration is singular, that is, $\xi^* = \xi'$, $\xi = \xi' + 1 - \sin y$ in the right side of expression (9). If the upper limit of integration is singular, i.e., $\xi^* = \xi''$, $\xi = \xi'' - 1 + \sin y$ in the right side of expression (9). Then, a good result for the above integration can be obtained by applying the conventional Gaussian quadrature.

2.3 BEM simulation of dynamic crack growth

According to Fedelinski [2], after discretization and integration, the matrix equation is obtained for time *t*, which is after *N* time steps

$$\boldsymbol{H}^{NN}\boldsymbol{u}^{N} = \boldsymbol{G}^{NN}\boldsymbol{t}^{N} + \sum_{n=1}^{N-1}(\boldsymbol{G}^{Nn}\boldsymbol{t}^{n} - \boldsymbol{H}^{Nn}\boldsymbol{u}^{n}) \tag{10}$$

New matrices, $\boldsymbol{A}^{NN}, \boldsymbol{B}^{NN}$, can be obtained by rearranging matrices $\boldsymbol{H}^{NN}, \boldsymbol{G}^{NN}$ according to boundary conditions. Matrix $\boldsymbol{A}^{NN}$ times unknown displacement and traction vector $\boldsymbol{x}^{N}$, and matrix $\boldsymbol{B}^{NN}$ times known displacement and traction vector $\boldsymbol{y}^{NN}$. Since matrices $\boldsymbol{H}^{Nn}, \boldsymbol{G}^{Nn}$ depend on the difference $N-n$, it is followed that $\boldsymbol{A} = \boldsymbol{A}^{NN}$. Therefore

$$\boldsymbol{A}\boldsymbol{x}^{N} = \boldsymbol{B}^{NN}\boldsymbol{y}^{N} + \sum_{n=1}^{N-1}(\boldsymbol{G}^{Nn}\boldsymbol{t}^{n} - \boldsymbol{H}^{Nn}\boldsymbol{u}^{n}) \tag{11}$$

Contrary to the case of a stationary crack the matrix A is not constant. New rows and columns should be added at each crack increment, but the elements in the origin A remain unchanged. If matrix A has been discomposed, only newly formed rows and columns need to be discomposed.

Dynamic stress intensity factor at each time step is computed by the method similar to that in reference [2].

3 Analysis and treatment of experimental data

Experimental data on dynamic crack growth of polystyrene given by Papadopoulos [5] are adopted in this paper. In reference [5], caustics were used to measure the dynamic stress intensity factors in the test. The material properties of polystyrene are: $E = 2.2\text{GPa}$, $\nu = 0.3$, $\sigma_y = 36\text{MPa}$ [7]. By rough estimation, if $K_I = 3\text{MPa}\sqrt{\text{m}}$, the size of crazing zone $R_0 = (K_I/\sigma_y)^2/(3\pi) \sim 0.001\text{mm}$, which is the same order as that of caustics D ~ 0.004mm. Therefore, the formulation (1) in reference [5] derived from perfect elastic materials may not be suitable for the case. In order to get the correct DSIFs, the finite element method is employed to analyze elasto-plastic crack, and the caustics are simulated to get the modified formulation for the case.

3.1 Finite element analysis for elasto-plastic crack

Considering a crack of mode I in elasto-plastic body, yielding takes place only within a very small zone around the crack tip. Displacement field around the crack tip is controlled by stress intensity factor. The size of outer boundary of FEM domain is taken as 30 times of plastic deformation zone so that condition of small range yielding can be satisfied.

In order to guarantee the accuracy of stress and strain fields around the crack tip, the size of smallest element is taken as 1/10000 of the domain. The number of all elements is 2000 in the solution domain.

The symmetry conditions of the crack of mode I can be written as

$$\left.\begin{aligned}\sigma_{12}(x_1, x_2 = 0) = 0\\ u_2(x_1, x_2 = 0) = 0\end{aligned}\right\}, \quad x_1 \geq 0 \tag{12}$$

which can be applied to the nodes in front of crack tip. Traction free boundary conditions are applied to the crack surfaces.

The von Mises yield criterion and isotropic hardening are used to model the elasto-plastic material.

In caustics, a shadow can be generated by reflection of light on a deformed surface. The diameter of the caustics is then related to stress intensity factor. In a view of mathematics, the caustic is a mapping from deformed surface to reference surface (Fig. 2).

Let (x_1, x_2) be a coordinate system on deformed surface of specimen, and the origin is at the crack tip. The deformed surface of specimen refracts light

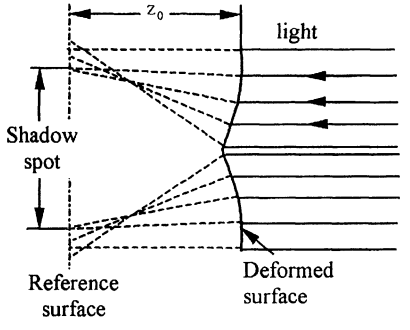

Figure 2. Shadow spot in caustics

onto coordinate system (X_1, X_2) on reference surface. Let z_0 be distance between deformed surface and reference surface. The mapping from (x_1, x_2) to (X_1, X_2) is given as follows:

$$X_\alpha = x_\alpha + 2z_0 \frac{\partial u_3(x_1, x_2)}{\partial x_\alpha} \tag{3}$$

where $u_3(x_1, x_2)$ is x_3 displacement of deformed surface, and subscript α denotes 1 or 2.

The process of simulation on caustics can be summed up as follows: Displacements of deformed surface and its mapping on reference surface are calculated from the elastic and elasto-plastic solutions of crack problem using FEM, and transverse diameters of shadows for both elastic and elasto-plastic materials are obtained. Thus, the ratio of two stress intensity factors corresponding to the two materials is obtained, $R = K'/K_I$, where K' is the SIF calculated by elastic solution and K_I is the SIF calculated by elasto-plastic solution with the same diameters of caustics.

3.2 Treatment of experimental data

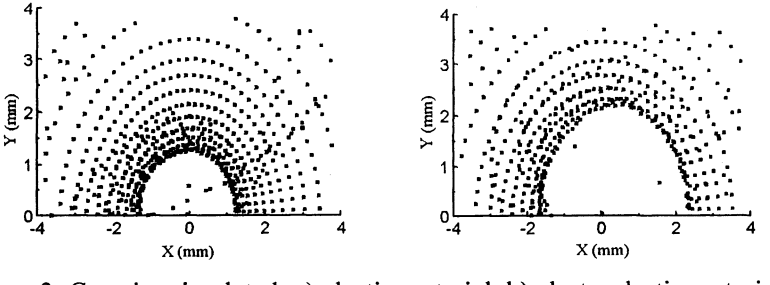

Figure 3: Caustics simulated: a) elastic material, b) elasto-plastic material

According to the conditions in the experiment of Papadopoulos [5], the

simulation of the caustics is carried out from 2 MPa$\sqrt{m}$ of SIF to 4 MPa$\sqrt{m}$. Figure 3a and 3b show caustics of elastic and elasto-plastic materials respectively when SIF is 3 MPa$\sqrt{m}$. It is apparent that the caustic size of elasto-plastic material is much larger than that of elastic material. Figure 4 shows that Ratio R varies with SIF K_I. The results show that when the size of nonlinear zone is not small enough to be able to be omitted, the error will be quite large if the data are still treated by elastic formulation. Figure 4 indicates that SIFs from the elastic results are several times of those from elasto-plastic results.

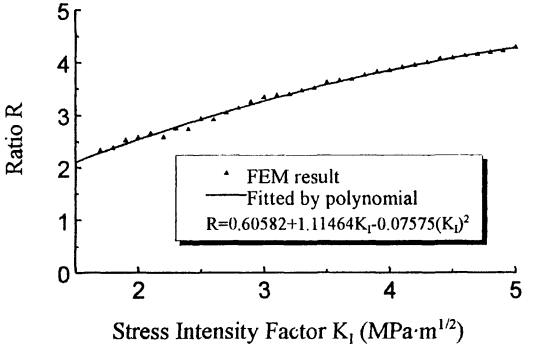

Figure 4: Ratio R varies with SIF K_I

4 Comparison of results

Boundary element method simulation on dynamic crack growth of polystyrene has been carried out in terms of geometry of specimen, loading, properties of material and velocities of crack growth in Papadopoulos' experiment[5].

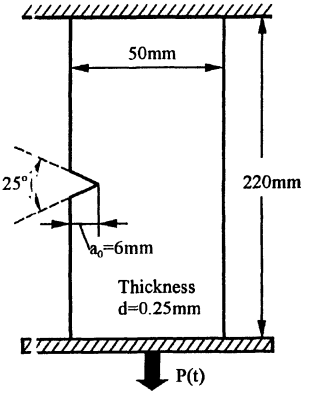

Figure 5: Geometry and boundary

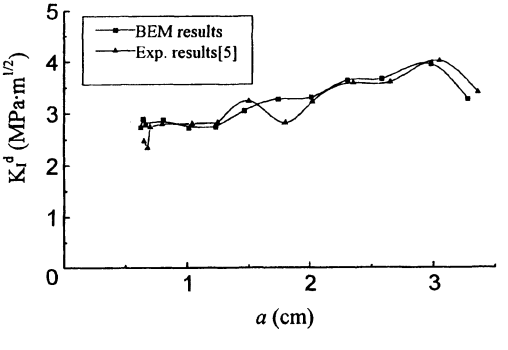

Figure 6: Experimental and computatinal results

The geometry of polystyrene specimen is $0.22 \times 0.05 \times 0.00025$ m with a V-cut in the middle of an edge. Upper boundary is fixed, and the other side is subjected to traction with strain rate $\dot{\varepsilon} = 10\,\mathrm{s}^{-1}$. The velocities of crack growth are taken from the data of Papadopoulos [5]. Dynamic stress intensity factors (DSIFs) are modified using the method mentioned above. Fig. 6 shows the comparison between experimental results and computational results. They agree quite well

5 Conclusion Remarks

In this paper time domain dual boundary element method has been studied and applied to the simulation of crack growth with non-uniform velocities. Finite element method has been used to analyze the stress and strain fields around the crack tip and the caustic method has been simulated to get the correct values of the dynamic stress intensity factors for the material of elasto-plastic. The results show:

1. Weakly singular integration method proposed in this paper is suitable to the straight-line elements in time domain dual boundary element method. High accuracy is achieved and the programming is quite simple.
2. TDBEM is suitable to simulate the crack growth with non-uniform velocities.

Acknowledgements

Financial support for the project from the National Natural Science Foundation of China, under grant No. 19772025 and the support from the Research Foundation of the Failure Mechanics Laboratory in Tsinghua University are gratefully acknowledged.

References

[1] Fedelinski P, Aliabadi M H, Rooke D P. Single-region time-domain BEM for dynamic crack problems. International Journal of Solids and Structures, 1995, 32(24): 3555~3571

[2] Fedelinski P, Aliabadi M H and Rooke D P. Time-domain DBEM for rapidly growing cracks. International Journal for Numerical Methods in Engineering, 1997, 40(9): 1555~1572

[3] Koller M G, Bonnet M, Madariaga R. Modelling of dynamical crack propagation using time-domain boundary integral equations. Wave Motion, 1992, 16(4): 339~366

[4] Gallego R, Dominguez J. Dynamic crack propagation analysis by moving singular boundary elements. Transactions of ASME, Journal of Applied Mechanics, 1992, 59(1): 158~162

[5] Papadopoulos G A. Effect of crack layer on dynamic crack propagation behaviour in polystyrene. Journal of Materials Science, 1992, 27(8):

2154~2160

[6] Zhou Zhihong, Yao Zhenhan and Wang Bo. Weakly Singular Integration in Time Domain DBEM. In: Yao Z and Tanaka M Eds. Proceedings of the Eighth China-Japan Symposium on BEM, Beijing: International Academic Publishers, 1998: 98~104

[7] Botsis J, Chudnovsky A, Moet A. Fatigue crack layer propagation in polystyrene. Part I: Experimental observation. International Journal of Fracture, 1987, 33(4): 263~276